



Electrochemical properties of palladium adlayers on Pt(1 1 0) substrates

J. Souza-Garcia^{a,b}, A. Berná^b, E.A. Ticianelli^a, V. Climent^{b,1}, J.M. Feliu^{b,*,1}

^a Instituto de Química de São Carlos, Universidade de São Paulo Av. Trab. São-carlense, 400 CP 780, São Carlos-SP, CEP 13560-970, Brazil

^b Instituto de Electroquímica, Universidad de Alicante, Apartado 99, Alicante, Spain

ARTICLE INFO

Article history:

Received 30 July 2010

Received in revised form 7 March 2011

Accepted 11 March 2011

Available online 29 March 2011

Keywords:

Pt(1 1 0)

Palladium deposition

Pd single layer

ABSTRACT

Palladium deposition on Pt(1 1 0) electrodes was studied. Differently from Pt(1 1 1) and Pt(1 0 0), first and further layers cannot be distinguished in this case only through the voltammetric behavior of hydrogen and anion adsorption. The potential of zero total charge (pztc) was determined as a function of the amount of deposited Pd using CO charge displacement experiments and voltammetric curves. The variation of the voltammetric charge due to hydrogen and anion adsorption has been followed during Pd deposition. The voltammetric charge between 0.06 and 0.4 V first decreases to a minimum, then increases and finally becomes stable, suggesting that the surface is finally covered with a Pd multilayer. The pztc and CO oxidation charge show similar behavior. CO oxidation, NO reduction and Cu UPD were used as probes to monitor Pd coverage. The potential of CO oxidation increases with Pd coverage while the potential of NO reduction decreases. Using the information obtained from Cu UDP and FTIR experiments it has been possible to determine when the first Pd single layer was completed and when a second (further) layer(s) starts to grow.

© 2011 Elsevier B.V. Open access under the [Elsevier OA license](#).

1. Introduction

The study of metal surfaces modified with selectively deposited adatoms is of great conceptual interest for the search of new materials with novel electrocatalytic properties. Such bimetallic surfaces may have different properties depending on whether the deposited amount is on the submonolayer, monolayer or multilayer level. These properties can be used to tailor the electrocatalytic activity of the electrode material for a particular electrochemical reaction.

The deposition of the foreign adatom can be made by underpotential deposition (UPD) [1–8] or by irreversible adsorption [9–16]. When deposition is made by UPD, the amount of deposited material is, most of the times, limited to one single layer. Moreover, the surface coverage of the foreign metal is usually a function of the applied potential. On the other hand, the irreversible adsorption method has the advantage that the adsorbed metal remains on the electrode surface with constant coverage in a wide range of potentials, even in the absence of the ions in solution [16].

The irreversible deposition of palladium on platinum single crystals has been studied for many years [17–21], this study being prompted by the interesting catalytic properties that this metal offers for many reactions. Work with palladium bulk single crystals has many difficulties, derived from the capacity of this metal to

absorb hydrogen. Then, the electrochemical response of palladium electrodes at potentials close to the onset of hydrogen evolution is dominated by the hydrogen absorption processes. Besides, this property of palladium prevents the use of the rather simple methods used for the preparation and handling of the electrodes of other metals like Pt, Au or Rh, including the flame annealing technique used for decontamination and reordering of the surface [18,21,22].

Palladium grows on platinum forming pseudomorphic adlayers that follow the crystallographic pattern of atoms in the substrate [19]. This allows the comparison of the reactivity of palladium deposits on platinum single crystals with that of the corresponding bulk crystals of palladium with the same orientation [23–25]. This comparison can shed some light on the processes of subsurface hydrogen and oxygen incorporation into the metal lattice [26,27]. The deposit is not restricted to a (sub)monolayer amount and multilayers can also be easily prepared. Such composite electrodes can be taken as substitutes for the bulk palladium electrodes, with hopefully similar catalytic properties but without the complication of hydrogen absorption [21]. However, it has been demonstrated that the first layer of deposited metal has particular properties, different from both Pt and Pd bulk electrodes, due to the interactions and electronic effects that platinum substrate atoms exert on the palladium adatoms [18,20].

Pd deposits can be managed in a larger potential range when compared to Pd single crystals, without the problems of hydrogen absorption or oxygen adsorption [17–21,28–32]. It is known that the cyclic voltammogram of submonolayer amounts of Pd

* Corresponding author. Tel.: +34 965 909 301; fax: +34 965 903 537.

E-mail address: juan.feliu@ua.es (J.M. Feliu).

¹ ISE member.

deposited on Pt(1 1 1) in H_2SO_4 has a pair of peaks around 0.23 V, corresponding to hydrogen and anions adsorption on palladium islands [20]. When increasing amounts of palladium are deposited, these peaks increase, while the characteristic features of hydrogen and anion adsorption on Pt(1 1 1) decrease. When a second layer of Pd starts to be formed, another pair of voltammetric peaks start to grow around 0.24–0.28 V and the first peak at 0.23 V decreases as the first monolayer is being covered. A Stranski–Krastanov growth mode has been described for this system, with an initial first monolayer growing in registry with the substrate, followed by a 3-D growth of the following layers [33].

Something similar happens with Pd deposition on Pt(1 0 0): the first layer has a pair of adsorption peaks around 0.17 V and when a second pair of peaks at 0.27 V appears, it means that a second palladium layer is being formed [18,21,34,35]. However, in this case, there is a higher tendency to form 3D islands and, although the deposition starts being pseudomorphic at low coverages, at medium or high coverages, 3D islands start to grow before the completion of the first layer [34]. However, Alvarez et al. showed that a deposit with a small excess of palladium in a second layer can be reorganized to achieve a rather perfect monolayer through the adsorption of a nitric oxide monolayer followed by its reductive stripping [34]. This process leads to the dissolution of excess palladium.

Different from the (1 1 1) and (1 0 0) cases, the deposition of Pd on Pt(1 1 0) does not have any characteristic peak that could serve as an indication of the amount of Pd deposited on the surface

[15,18,21], and no reports of the identification and electrochemical characterization of the first Pd monolayer on Pt(1 1 0) have been made. Although beyond the scope of the present paper, understanding the processes of subsurface hydrogen and oxygen incorporation can benefit from the knowledge of the electrochemical behavior of palladium adlayers on this basal plane of platinum. In this respect Pt(1 1 0) substrates have been proposed to incorporate subsurface hydrogen and subsurface oxygen that could be most important to understand the reactivity of this open surface [26,27]. In this paper, deposition of palladium on Pt(1 1 0) has been followed by careful voltammetric experiments, including charge displacement, structure sensitive reactions and spectroscopic measurements.

2. Experimental

Platinum electrodes were prepared from small single crystal beads following the method developed by Clavilier [36]. Once oriented, the single crystal beads were fixed, cut till the bead maximum diameter, polished down to 0.25 μm and finally annealed. Prior to each experiment the hemispherical Pt electrode was flame annealed, cooled down to room temperature under $\text{Ar} + \text{H}_2$ atmosphere and transferred to a cell with a droplet of water in equilibrium with this mixture of gases to protect its surface from ambient contamination.

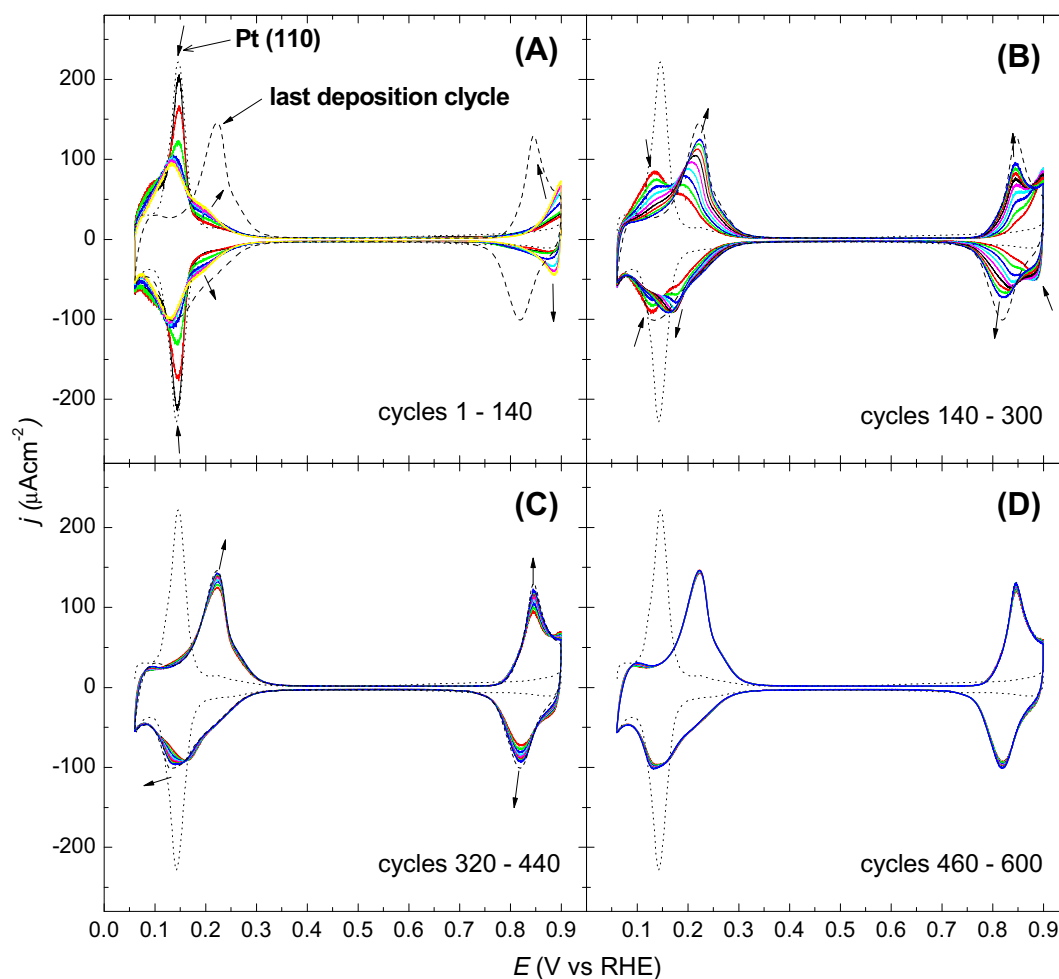


Fig. 1. Palladium deposition on a Pt(1 1 0) electrode. $2.5 \times 10^{-6}\text{M}$ PdSO_4 in 0.1 M H_2SO_4 . Scan rate 50 mVs^{-1} . Dot line: Pd-free Pt(1 1 0). Dash line: Pt(1 1 0) with Pd multilayers. (A) Cycles 1 – 140; (B) cycles 160–300; (C) cycles 320–440; (D) cycles 460–600.

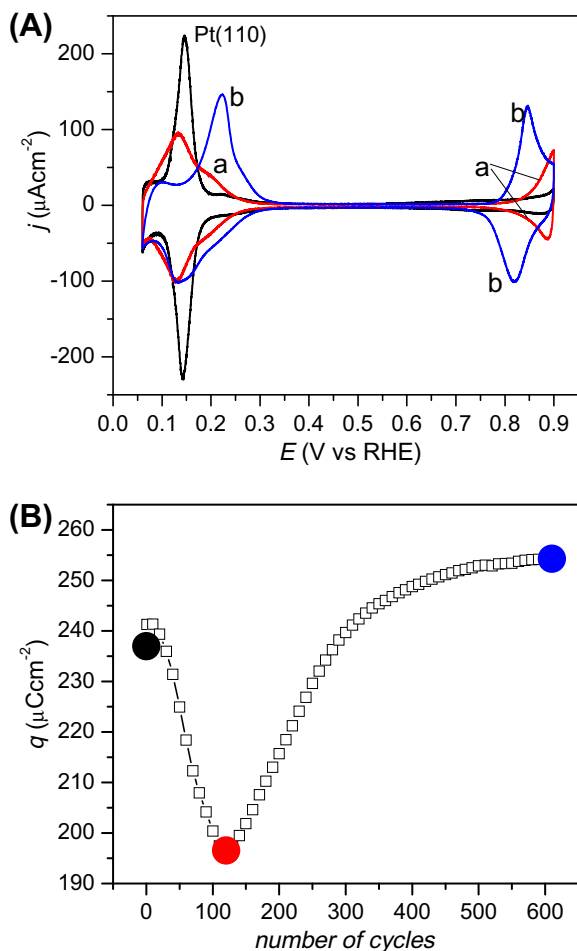


Fig. 2. (A) Voltammograms of palladium modified Pt(110) electrodes with different palladium deposits. (B) Total charge (average between positive and negative sweeps) integrated between 0.06 and 0.4 V from the voltammograms presented in Fig. 1 for Pd deposition on Pt(110) electrode. The points mark the position of the three selected states in Fig. 2A.

Before the preparation of palladium layers, the characteristic voltammogram of Pt(110) was recorded to confirm the cleanliness and order of the surface [37,38]. Palladium was deposited electrochemically in a deposition cell. The electrochemical deposition was carried out in a 0.1 M H_2SO_4 solution with $1\text{--}5 \times 10^{-6}$ M PdSO_4 , by means of continuous cycling between 0.06 and 0.80 V at 50 mVs^{-1} . After palladium deposits were made, the electrode was rinsed with water and transferred to a cell free of palladium for charge displacement, CO stripping, NO reduction, Cu UPD and FTIR experiments. For all the cells in this work a platinum wire was used as counter electrode and a reversible hydrogen electrode (RHE) was used as reference electrode. For CO charge displacement experiments, a glass tube was used to dose CO (Air liquide, N48) near the electrode surface, as described elsewhere [39,40]. NO adsorbed layer was obtained by the contact of the electrode with a nitrite solution as described in ref [41–44]. Underpotential deposition (UPD) of copper was carried out in 0.1 M H_2SO_4 and 2×10^{-3} M CuSO_4 .

Spectroelectrochemical experiments were performed with a Nicolet Magna 850 spectrometer equipped with a MCT detector. The spectroelectrochemical cell was provided with a prismatic CaF_2 window bevelled at 60° . Spectra shown in this work are presented as absorbances, according to $A = -\log(R/R_0)$ where R and R_0 are the reflectance corresponding to the single beam spectra obtained at the sample and reference potentials, respectively. Reference spectra were collected at 0.1 V with the surface free of CO.

Solutions were prepared from concentrated sulfuric acid (suprapur, Merck), palladium sulfate (p.a., Sigma–Aldrich), copper (II) sulfate pentahydrate (p.a., Merck), sodium nitrite (Sigma–Aldrich) and ultra-pure water (Elga–Vivendi or Milli Q, $18.2 \text{ M}\Omega \text{ cm}$). The cell and all glassware were cleaned in a potassium permanganate solution for 12 h, followed by rinsing with water and a solution of hydrogen peroxide and sulfuric acid. Finally, everything was repeatedly rinsed and boiled with ultra-pure water. The measurements were performed at room temperature and in the hanging-meniscus configuration. The solutions were deaerated with Argon (N50, Air Liquide).

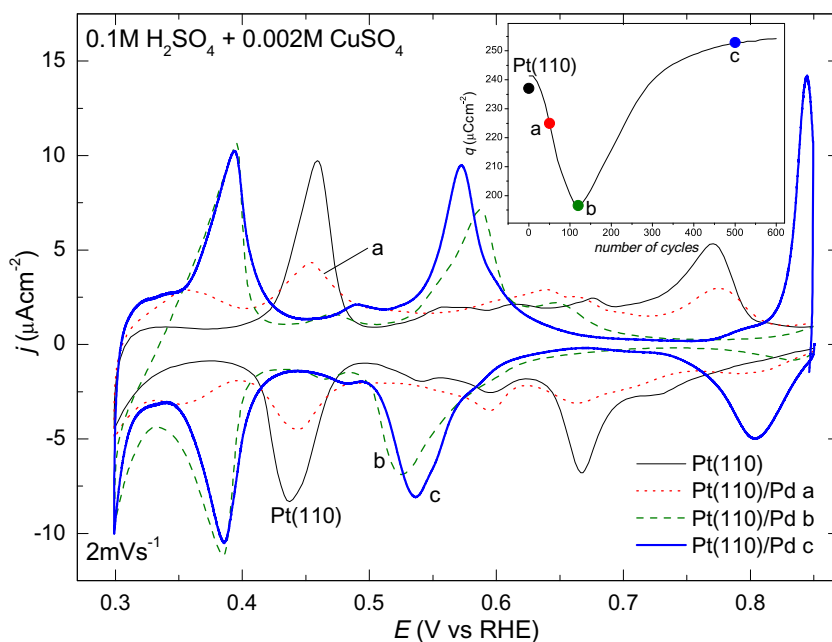


Fig. 3. Voltammograms of Cu UPD on palladium modified Pt(110) electrodes with different palladium deposits. Inset: total charge evolution as shown in Fig. 2B and the charges corresponding to the three deposits in the main figure. Test solution 0.1 M H_2SO_4 and 0.002M CuSO_4 . Scan rate 2 mVs^{-1} .

3. Results and discussions

To follow voltammetrically the different stages during Pd deposition, a low concentration of PdSO_4 was used, 2.5×10^{-6} M, making the deposition reasonably slow. At higher Pd^{2+} concentrations, the deposition became too fast and it was not possible to accurately observe the evolution of the voltammetric profile with time. Smaller concentrations do not produce significant voltammetric changes.

Fig. 1 shows the evolution of palladium deposition on Pt(1 1 0) (one curve for each 20 cycles). It is possible to see that the peaks corresponding to hydrogen and anions adsorption on Pt(1 1 0), around 0.14–0.15 V, decrease as Pd is being deposited, but no peaks that could be clearly attributed to adsorption processes on Pd can be distinguished from the base voltammetry of the platinum substrate, as it is the case for Pd deposition on Pt(1 1 1) and Pt(1 0 0) [20,34]. However, four steps can be identified during Pd deposition: (1) Pt(1 1 0) adsorption peaks decrease and shift to 0.13 V and the currents at the region of 0.2 V and 0.85–0.9 V increase (cycles 1 – 140 – Fig. 1A); (2) the pair of peaks at 0.13 V decreases until it disappears, while new pairs of peaks appear and increase, one at 0.19 V, shifting to more positive potentials in the positive scan and to more negative potentials in the negative scan, and a second one at 0.85 V, shifting to less positive potentials in the negative scan (Cycles 160 – 300 – Fig. 1B); (3) peaks at 0.22 and 0.85 V in the positive scan and 0.82 V in the negative scan increase

and the peak at 0.16 V in the negative scan shifts to more negative potentials (Cycles 320 – 440 – Fig. 1C); (4) the voltammetric profile stabilizes and no more significant changes can be observed (Cycles 460 – 600 – Fig. 1D). Other observation is that two isopotential points can be seen in the cathodic scan: the first at low coverages, at 0.17 V and the second at higher coverages, at 0.19 V. Isopotential points appear in the voltammogram when the total current can be considered a linear combination of two or more competitive processes.

The information obtained from the voltammetric results is not enough to determine when a first Pd layer is complete or when the deposition achieves the multilayer level. To try to understand the changes in the voltammogram during Pd deposition, the voltammetric charges, between 0.06 and 0.4 V, were measured and are shown in Fig. 2B. The charge represented corresponds to the average between the positive and negative cycles. The total charge initially decreases until a minimum point is achieved. Then, the charge starts to increase and, finally, after many cycles, it remains stable. This minimum charge point seems to indicate a particular state in the properties of the bimetallic electrode surface, that could be related with the completion of the first Pd layer. However, more information is necessary to clarify this point.

The voltammograms corresponding to three characteristic stages during Pd deposition are summarized in Fig. 2A, together with the blank voltammogram for Pt(1 1 0). The charge values integrated between 0.06 and 0.4 V for these particular stages of

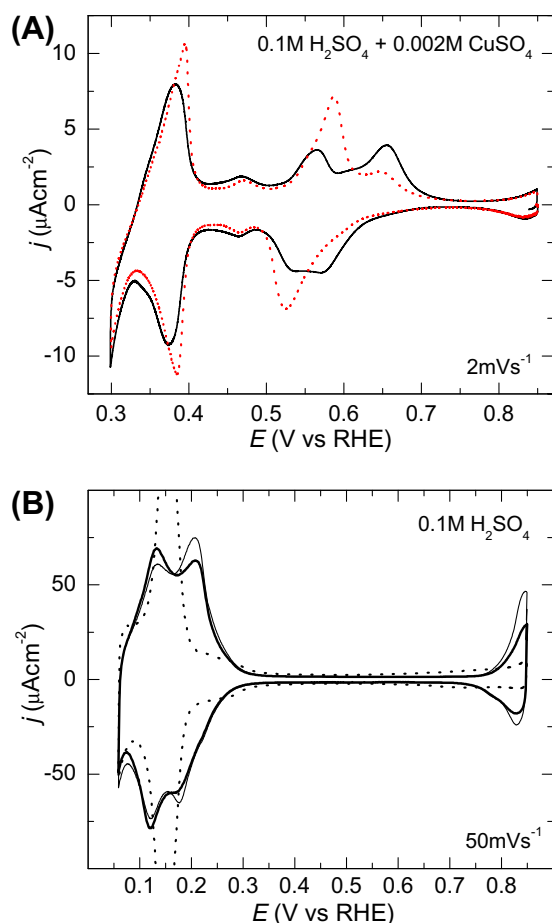


Fig. 4. (A) Voltammograms of Cu UPD on palladium modified Pt(110) with minimal total charge after fast (solid thin line) and slow (dotted line) deposition. Test solution 0.1 M H_2SO_4 and 0.002M CuSO_4 . Scan rate 2 mVs^{-1} . (B) Voltammograms of Pt(1 1 0) (dotted line) and Pd modified Pt(1 1 0) after fast deposit before (solid thin line) and after (bold line) Cu UPD. Test solution 0.1 M H_2SO_4 . Scan rate 50 mVs^{-1} .

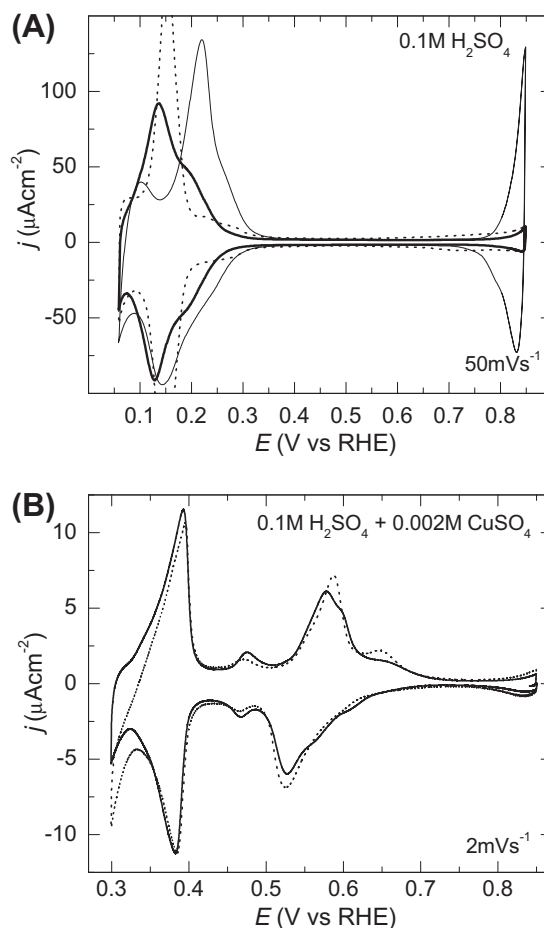


Fig. 5. (A) Voltammograms of Pt(1 1 0) (dotted line) and Pd modified Pt(1 1 0) before (solid thin line) and after (bold line) NO reduction. Test solution 0.1 M H_2SO_4 . Scan rate 50 mVs^{-1} . (B) Voltammograms of Cu UPD on palladium modified Pt(1 1 0) with minimal total charge (dotted line) and the same electrode as (A) after NO reduction. Test solution 0.1 M H_2SO_4 and 0.002M CuSO_4 . Scan rate 2 mVs^{-1} .

the Pd deposition process are marked in the curve presented in Fig. 2B.

Since hydrogen UPD has revealed insufficient to provide an unambiguous identification of the structure of the Pd adlayer, and more specifically, to provide an indication of the completion of the first Pd layer, Cu UPD, NO reduction and CO oxidation were used as additional probes that can provide information sensitive to the structure of the deposit.

3.1. Copper UPD

Cu UPD has been used before to characterize palladium single crystals [25] or Pt Pd alloys [45]. Underpotential deposition of copper on Pt(1 1 0) takes place on two different steps: one between 0.85 and 0.5 V, with a reduction peak at 0.67 V and an oxidation peak at 0.77 V, and another between 0.5 and 0.35 V, with well defined peaks at 0.44–0.46 V [1,46]. Each one of these processes is related to the deposition of a complete Cu layer. On Pd(1 1 0), the same two processes are observed, but with different peak potentials: 0.54–0.57 V for the first layer and 0.38–0.39 V for the second layer [1,25]. In this way, Cu UPD can be used to analyze the surface and to determine when Pt(1 1 0) sites are completely covered by Pd.

Fig. 3 shows the voltammetric profile of Cu UPD on Pt(1 1 0) and three different Pd coverages as indicated in the inset. When the electrode is decorated with a small amount of palladium, indicated as 'a' in the figure, the peaks corresponding to Cu UPD on Pt(1 1 0) sites decrease, but are still present, and a second pair of peaks at 0.35 V appears, indicating the presence of both Pt and Pd atoms on the surface. When the Pd deposition attains the minimum total charge of hydrogen and anion adsorption in the voltammogram, as described before, the peaks corresponding to Cu UPD on Pt completely disappear, curve 'b'. At this point, only the peaks related to Cu deposition on Pd atoms are observed, suggesting that the Pt(1 1 0) surface is completely covered with Pd atoms. Besides the peaks just mentioned, some non-well-defined processes, involving small charge density values, can also be observed in the potential region between 0.6 and 0.7 V. Although the origin

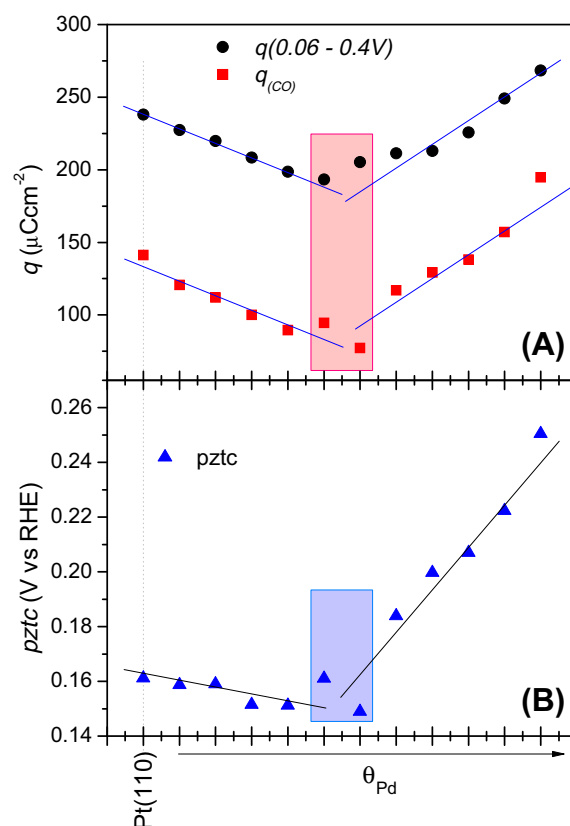


Fig. 7. (A) Charge displaced by CO at 0.1 V in 0.1 M H_2SO_4 ($q(\text{CO})$) and total charge between 0.06 and 0.4 V of Pt(1 1 0) with different palladium coverage (θ_{Pd}). (B) Potential of zero total charge (pztc) of the same electrodes. Rectangles show the points that correspond to the minimum charge.

of these processes is difficult to assign with only the present electrochemical information, they are most probably related with the Cu UPD on defect sites either on the Pt surface, on the Pd adlayer

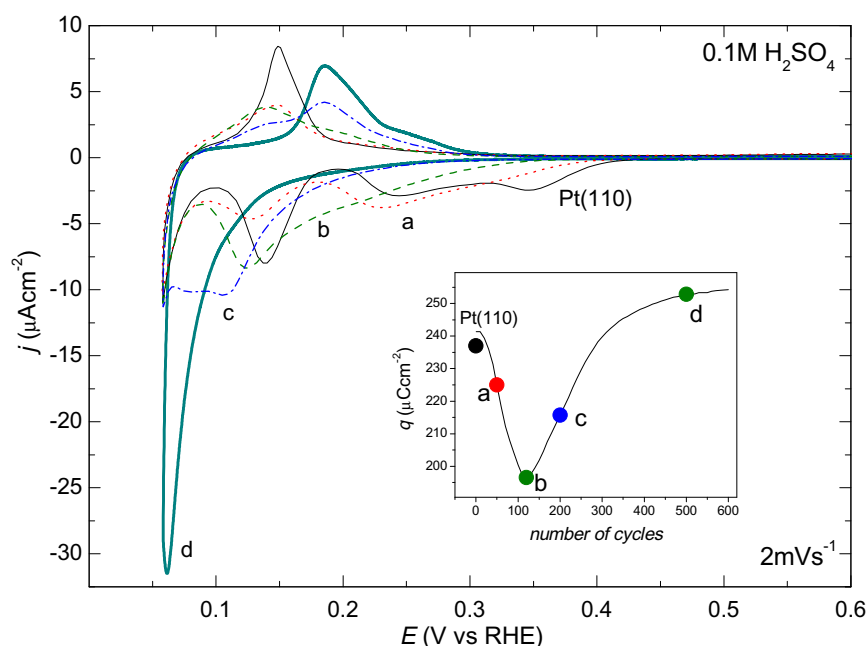


Fig. 6. Reduction of a NO adsorbed layer on Pt(1 1 0) (solid thin line) and four different palladium coverages, as indicated in the inset. Test solution 0.1 M H_2SO_4 . Scan rate 2 mVs^{-1} .

or even on the edges of Pd islands. Finally, if the coverage of Pd is higher than that corresponding to the minimum, Cu UPD has always the same profile, indicated as 'c', with no contribution of Pt(1 1 0) sites for Cu UPD.

The results presented at Fig. 3 suggest that the first palladium layer is complete when the total charge of the voltammogram between 0.06 and 0.4 V is minimal. However, this observation is true only if the deposition is made slowly, in a very diluted Pd^{2+} solution, as described in Fig. 1. When palladium deposition is done faster, despite the voltammetric profile being very similar at the minimal charge (Fig. 2, curve a), Cu UPD profile suggests that in this case the palladium layer is not as uniform as that previously described. Fig. 4A shows one result obtained with a 5×10^{-6} M Pd^{2+} solution. As mentioned above, the peak at 0.65 V in the voltammogram corresponding to the adlayer deposited faster can be related to Cu UPD on defects sites or on Pt atoms still available on the surface, electronically modified by the presence of the Pd.

Another observation that should be made is that the deposition and oxidation of Cu atoms on the Pd modified Pt(1 1 0) surface can either modify the adlayer or even remove Pd atoms. Fig. 4B shows the blank voltammogram for a Pd deposit with an initial state (before Cu UPD) with total charge located after the minimum, before and after Cu UPD. Cu UPD voltammetric profile is similar to the one described before (Fig. 3, curve c), but the blank voltammogram of

the electrode after Cu UPD shows that Pd atoms were removed from the surface or were reorganized, since it shows a profile that resembles the one obtained at an earlier stage in the Pd deposition.

3.2. NO reduction

NO reduction has also been studied as another probe reaction sensitive to the structure but also because formation and elimination of a NO adsorbed layer has been proved beneficial to obtain a well ordered Pd monolayer on Pt(1 0 0) [34]. It was shown by Álvarez and coworkers [34] that the deposition of a second Pd layer on Pt(1 0 0) starts before the first layer is completed and that a good method to obtain a complete Pd first layer is to reduce a NO adsorbed layer on an electrode initially covered with a Pd coverage slightly higher than the monolayer.

A NO adsorbed layer can be obtained by the contact of the electrode at open circuit with a nitrite solution in water or in acid media. In acid media the equilibrium of HNO_2 disproportionation favors NO formation and the attained coverage of NO adsorbed layer on the electrode is higher [47]. When nitrite solution is prepared in water, the concentration of NO in solution is lower and the coverage of NO on the electrode surface is smaller. In the present work a complete saturate layer of NO on Pt(1 1 0), with a coverage of 0.7, comparable to that reported in Ref [48], was obtained after

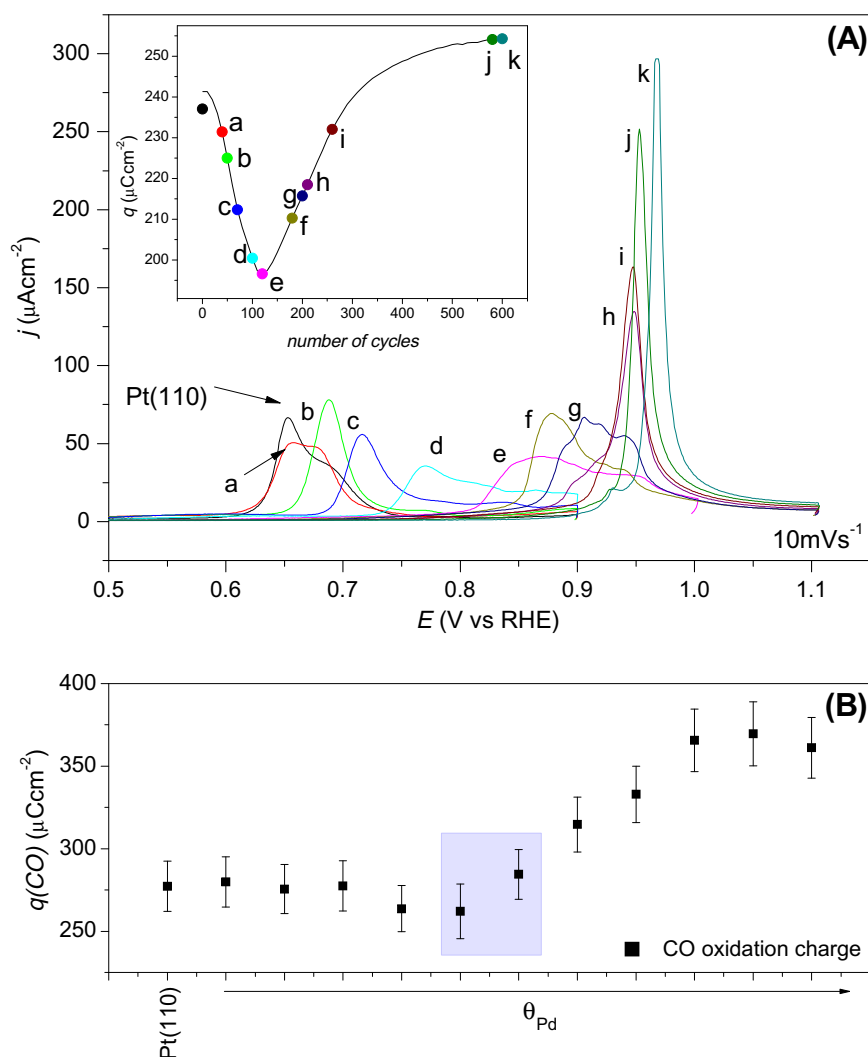


Fig. 8. (A) CO stripping of palladium modified Pt(1 1 0). The integrated charge in the blank voltammogram for each of the deposits is shown in the inset together with the curve of Fig. 2B. (B) CO oxidation charge from (A).

the contact of the electrode with a solution of 10^{-2} M NaNO_2 in 0.1 M H_2SO_4 . If a 1 M NaNO_2 in water was used, only half layer of NO was obtained (0.35) after 6 min. NO coverages are calculated from the reductive charge integrated in the voltammetric stripping, corrected from the readsorption of a hydrogen monolayer that takes place after NO desorption [49].

As observed for Pd deposits on Pt(1 0 0) [34], the adsorption and elimination of a saturated NO adsorbed layer, obtained from an acidic nitrite solution, on Pd modified Pt(1 1 0) exerts significant changes in the voltammetric response of the adlayer. Fig. 5A shows the blank voltammogram of a Pd modified Pt(1 1 0) electrode, before and after NO reduction. After NO reduction the voltammetric profile changes from one that indicates a high Pd coverage to one that agrees with the Pd coverage with minimum charge (Fig. 2, curve a). Also, the profile of NO reduction was similar to the one observed for Pd coverage with minimum charge (Fig. 6). Cu UPD after NO reduction also shows that the electrode surface is similar to the one obtained at the minimum charge, even more ordered, since the shoulder at 0.65 V is almost absent (Fig. 5B). Since the reduction of the NO layers adsorbed in acid NaNO_2 solutions removes Pd atoms from the surface, to study the activity of Pt(1 1 0) with different amounts of Pd on the surface for this reaction, NO adlayers were prepared by contact of the electrode with NaNO_2 solution prepared in water. The results are presented in Fig. 6 and show that, as palladium coverage increases, NO reduction shifts to more negative potentials. No significant changes on the voltammetric profile were observed after NO reduction, indicating that under these conditions adsorption of NO does not remove Pd atoms.

3.3. Charge displacement experiments and CO stripping

The charges displaced by CO at 0.1 V, on electrodes with different palladium coverage are presented in Fig. 7A. For the unmodified (1 1 0) surface, nearly $150 \mu\text{C cm}^{-2}$ are displaced at 0.1 V, corresponding to the charge of 1 ML of hydrogen on the (1 × 1) surface, in agreement with literature data [50]. When Pd is deposited on the surface, the hydrogen coverage at 0.1 V decreases, reaching a minimum value around $75 \mu\text{C cm}^{-2}$. It is possible to see that the occurrence of the minimum displaced charge is in agreement with a coverage corresponding to the minimum total charge integrated between 0.06 and 0.4 V.

The charges displaced by CO are useful to determine the potential of zero total charge (pztc) of the electrodes [20,39,51]. This potential can be found from the curve obtained by subtracting the charge displaced by CO ($q_{\text{dis}(\text{ECO})}$) from the charge integrated from the voltammogram, following the equation [39]:

$$q(E) = \int_{E_{\text{CO}}}^E \frac{j(E)}{\nu} dE - q_{\text{dis}(E_{\text{CO}})} \quad (1)$$

where E_{CO} is the potential of CO displacement and ν the scan rate. The results for the pztc (average between the values obtained from the positive and negative scans) are presented in Fig. 7B. A decrease in the pztc is observed for small coverages, with a minimum in pztc coinciding with the minimum in the displaced charge at 0.1 V and also with the minimum in the integrated charge. This result contrast slightly with the trend published previously for polycrystalline platinum [52], where almost no changes are observed when platinum is compared with palladium, although it agrees with the results observed for the other basal planes of platinum. A decrease of pztc at submonolayer palladium amounts has also been observed for Pd/Pt(1 1 1) and interpreted as a result of the strong interaction of sulfate anions with the Pd(1 1 1) surface [30].

These results show the same tendency for all cases, with the minimum in the integrated charge always corresponding to the

same palladium coverage, indicating that at this stage a first complete Pd layer is present.

The subsequent oxidation of CO can also shed some light on the Pd adlayer properties. Fig. 8A shows the CO stripping, after complete surface blocking in the displacement experiment, on different palladium covered Pt(1 1 0) electrodes. The oxidation is shifted to more positive potentials as the amount of palladium increases. These results suggest that CO adsorbed on the Pd adlayer is oxidized at more positive potentials than CO adsorbed on Pt. The charge of CO oxidation is given in Fig. 8B. As in the other cases, there is a change in the behavior when the palladium coverage gives the minimum total voltammetric charge. To understand this change, some FTIR experiments were carried out.

3.4. FTIR experiments

Two different experiments were done using FTIR. The first one was to identify CO adsorption on Pt and Pd, at $E = 0.1$ V, that appear at different wavenumbers, that reflect the different bonding mode

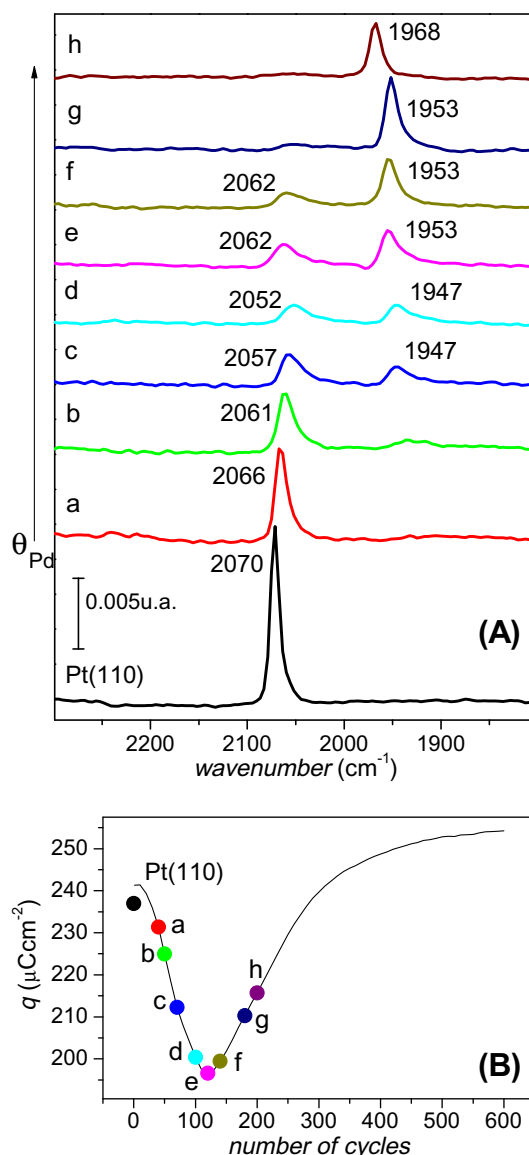


Fig. 9. (A) In situ infrared spectra collected at 0.10 V for a saturated CO adlayer on different palladium coverage; reference potential: 1.0 V; test solution: 0.1 M H_2SO_4 . (B) Same as Fig. 2B and the symbols indicate the corresponding charge of the Pd coverage of each spectra shown in (A).

of CO with the substrate atoms. The results are presented in Fig. 9. The second aspect was to follow the displacement of the CO oxidation potential caused by palladium modification, in which spectra were recorded (1 spectrum every 5 mV) during CO oxidation (done at 1 mVs^{-1}). Fig. 10 shows the results for Pt(1 1 0) and for three different palladium modified Pt(1 1 0): before the minimum charge, at the minimum charge and after the minimum charge.

From the spectroelectrochemical results presented in Fig. 9 it is possible to see that the peak at 2070 cm^{-1} , related to the vibration of CO adsorbed on-top on Pt(1 1 0) ($\text{CO}_{\text{L-Pt}}$) [53] decreases and shifts to lower wavenumbers as the coverage of Pd increases, until the Pd coverage attains the value corresponding to the minimum charge. When this coverage is attained, this band jumps to higher wavenumbers (2062 cm^{-1}) and remains at this position until it disappears at high Pd coverages. According to Gómez et al. [15], CO molecules adsorb on Pt(1 1 0) covered with Pd multilayers preferentially at bridge configuration ($\text{CO}_{\text{B-Pd}}$) but some linear adsorbed CO ($\text{CO}_{\text{L-Pd}}$) is also seen. The two species are seen at 1947 and 2039 cm^{-1} , respectively [15]. We can explain the spectroscopic observations of Fig. 9 in the following way. When only a few Pd atoms are deposited on the Pt(1 1 0) surface, there are no big islands of Pd, and the probability of finding two adjacent Pd atoms that can accommodate a bridge CO is small. In this way, CO could adsorb only linearly on Pd at small coverage. Since the bands of $\text{CO}_{\text{L-Pt}}$ and $\text{CO}_{\text{L-Pd}}$ are close to each other, with the latter at lower wavenumbers, when $\text{CO}_{\text{L-Pd}}$ band starts to grow, these two bands merge and the result is equivalent to a shift to lower wavenumbers. Another contribution to the bandshift of $\text{CO}_{\text{L-Pt}}$ caused by palladium deposition is related to the effect of dipole coupling on the

CO vibrational frequency. When the CO coverage is high on the Pt(1 1 0), the lateral interaction within the adlayer increases the vibrational frequency of this species [53]. When Pd atoms are present on the surface, the CO islands will be disrupted and the lateral interaction within CO molecules will decrease, causing a red shift of the $\text{CO}_{\text{L-Pt}}$ band. When Pd coverage corresponds to the minimum charge the band jumps to 2062 cm^{-1} . According to the results showed previously, this situation corresponds to the completion of the first layer of Pd. The sudden blueshift of the band reinforces this conclusion, since, if there were a $\text{CO}_{\text{L-Pt}}$ contribution to this band, it would be expected to keep shifting to lower wavenumbers, following the same tendency observed at lower Pd coverages. However, after the completion of the Pd layer, this band would be related only to $\text{CO}_{\text{L-Pd}}$ species. As mentioned before, the interaction of CO molecules displaces the vibrational frequencies to higher wavenumbers, in agreement with the observations of Fig. 9. With more than one layer of palladium the $\text{CO}_{\text{L-Pd}}$ peak decreases, but its frequency does not change. When multilayers of Pd are present, almost no contribution of this band is observed, as expected in agreement with Ref [15].

CO needs more than one Pd atom on the neighborhood to adsorb at bridge configuration. In this way, Pd coverage must be high enough to allow this configuration and that is what is seen in Fig. 9. As discussed previously, the band corresponding to $\text{CO}_{\text{B-Pd}}$ is not observed when only a few Pd atoms are on the surface. As more Pd atoms are deposited, this band appears and increases with coverage, but no significant changes in its wavenumber are observed at intermediate Pd coverages. However, with the maximum coverage depicted in Fig. 9h, which would consist of Pd multilayers, the

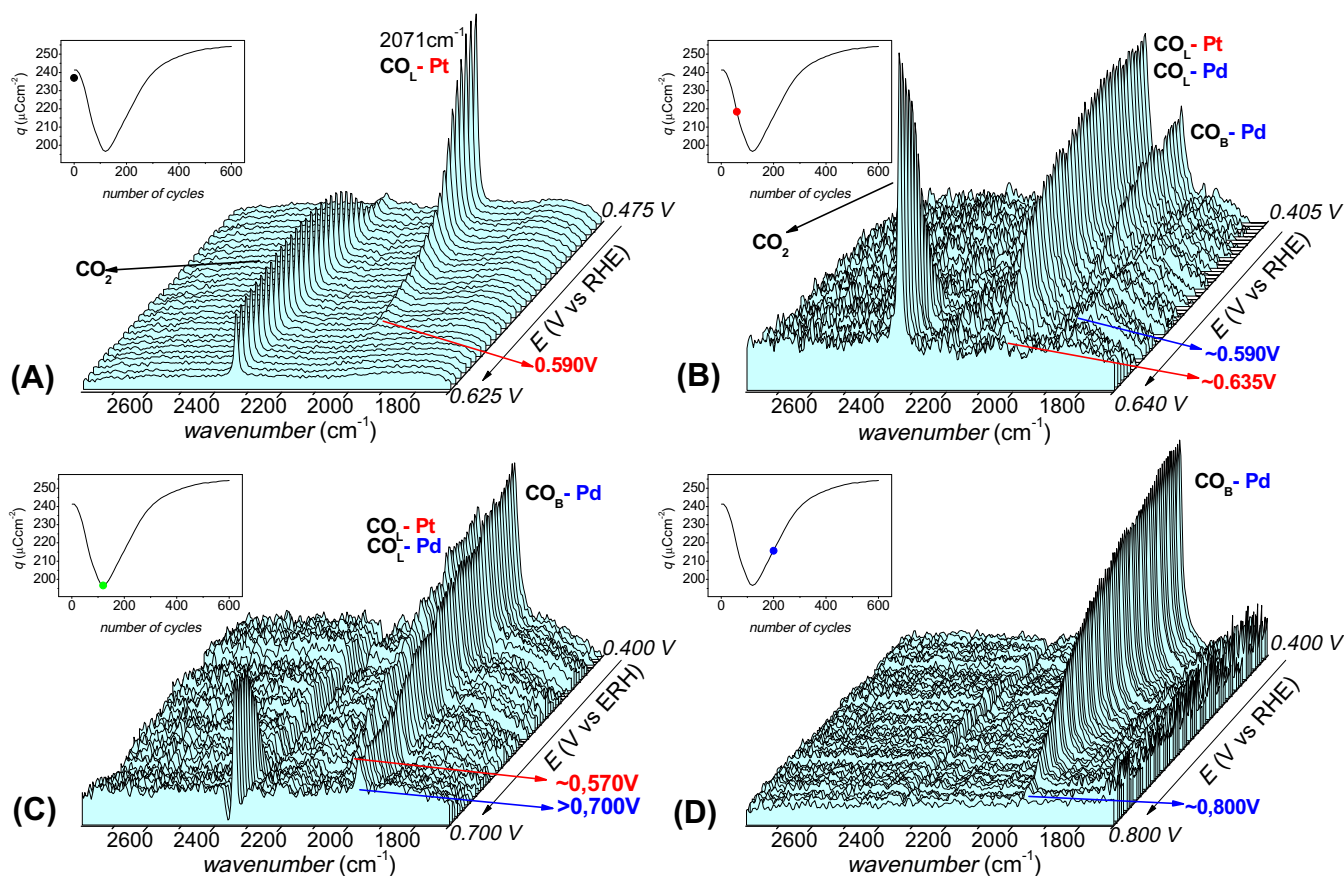


Fig. 10. Series of infrared spectra obtained during CO stripping: (A) Pt(1 1 0); (B) Pd modified Pt(1 1 0) with total charge before minimum; (C) Pd modified Pt(1 1 0) with minimum total charge; (D) Pd modified Pt(1 1 0) with total charge after minimum (only Pd on the electrode surface). Insets in B–D show the total charge of each Pd deposit. Test solution: $0.1 \text{ M H}_2\text{SO}_4$, scan rate 1 mVs^{-1} , 1 spectra each 5 mV , resolution 8 cm^{-1} .

$\text{CO}_{\text{B-Pd}}$ band is again bluishifted to 1968 cm^{-1} , indicating that, at this stage, compact islands of CO start being formed, with the dipole–dipole coupling between CO molecules causing this frequency to increase.

In Fig. 10A it is possible to see the peak corresponding to $\text{CO}_{\text{L-Pt}}$ at 2071 cm^{-1} . This peak decreases as the potential increases, indicating the oxidation of CO, and a second peak appears at 2345 cm^{-1} , corresponding to CO_2 formed from CO oxidation. CO oxidation is complete around 0.59 V. When the electrode surface is modified with palladium (an amount such that the total charge is not at the minimum yet, what means that both Pt and Pd atoms are available on the surface), two peaks can be seen at 0.4 V (Fig. 10B), the one corresponding to $\text{CO}_{\text{L-Pt}}$ and $\text{CO}_{\text{L-Pd}}$ and another one corresponding to $\text{CO}_{\text{B-Pd}}$. Both peaks decrease as a result of CO oxidation with the increase of the potential, but the peak of $\text{CO}_{\text{B-Pd}}$ disappears at lower potentials than the peak of $\text{CO}_{\text{L-Pt}}$ and $\text{CO}_{\text{L-Pd}}$. We can suggest that $\text{CO}_{\text{B-Pd}}$ is oxidized at lower potentials than the $\text{CO}_{\text{L-Pt}}$ or $\text{CO}_{\text{L-Pd}}$, or both, or that CO can migrate on the electrode surface and, as $\text{CO}_{\text{L-Pt}}$ is oxidized, $\text{CO}_{\text{B-Pd}}$ and $\text{CO}_{\text{L-Pd}}$ migrate to free Pt sites and are oxidized there. When the palladium coverage is about one single layer (Fig. 10C), the opposite happens, i.e., the peak of $\text{CO}_{\text{B-Pd}}$ is the last one to disappear, suggesting that $\text{CO}_{\text{L-Pd}}$ is oxidized sooner than $\text{CO}_{\text{B-Pd}}$, which is more stable. Finally, when there is only Pd atoms on the electrode surface (Fig. 10D) the potential for the total CO oxidation is higher than in the previous cases.

These results show that the presence of Pd does not improve CO oxidation, in agreement with the CO stripping experiments showed in Fig. 8. FTIR results showed that, when the first Pd single layer is complete, CO is adsorbed in both bridge and linear configurations, differently from what happens on Pt(1 1 0), that adsorbs CO only in linear configuration. In this way, on the Pd-free Pt(1 1 0), the coverage of CO is higher than for Pt(1 1 0) with a Pd single layer. This agrees with the decrease of the CO charge at this point (Fig. 8B). As the coverage of Pd increases to more than a single layer, Pd atoms can probably be forming some islands on the electrode surface, leaving more Pd atoms available for CO adsorption, justifying the increase of CO charge after the first layer is complete.

4. Conclusion

When done slowly in a very diluted solution, the deposition of Pd atoms on the Pt(1 1 0) surface presents some characteristic changes when the total charge of hydrogen and anions adsorption has a minimum value. At this point, using Cu UPD and NO reduction experiments, it was possible to show that a Pd single layer was complete without free Pt atoms exposed on the surface.

FTIR experiments showed that Pd does not improve CO oxidation on Pt(1 1 0) and that for Pt(1 1 0) with a single Pd layer CO adsorbs both bridge and linearly bonded, indicating that it has properties intermediate to Pt(1 1 0) and Pd(1 1 0) surfaces.

Acknowledgements

Financial support from the Generalidad Valenciana (Spain) through Project Prometeo/2009/045 and CAPES and CNPq (Brazil) are gratefully acknowledged.

References

- [1] M.S. Zei, *Zeitschrift für Physikalische Chemie – International Journal of Research in Physical Chemistry & Chemical Physics* 208 (1999) 77.
- [2] S.J. Hsieh, A.A. Gewirth, *Langmuir* 16 (2000) 9501.
- [3] O. Endo, N. Ikemiya, M. Ito, *Surface Science* 514 (2002) 234.

- [4] J. Okada, J. Inukai, K. Itaya, *Physical Chemistry Chemical Physics* 3 (2001) 3297.
- [5] P.M. Rigano, C. Mayer, T. Chierchie, *Electrochimica Acta* 35 (1990) 1189.
- [6] N. Markovic, P.N. Ross, *Langmuir* 9 (1993) 580.
- [7] N. Markovic, P.N. Ross, *Journal of Vacuum Science & Technology A – Vacuum Surfaces and Films* 11 (1993) 2225.
- [8] T. Chierchie, C. Mayer, *Electrochimica Acta* 33 (1988) 341.
- [9] J.F.E. Gootzen, P.G.J.M. Peeters, J.M.B. Dukers, L. Lefferts, W. Visscher, J.A.R. van Veen, *Journal of Electroanalytical Chemistry* 434 (1997) 171.
- [10] R. Hoyer, L.A. Kibler, D.M. Kolb, *Electrochimica Acta* 49 (2003) 63.
- [11] J. Tang, M. Petri, L.A. Kibler, D.M. Kolb, *Electrochimica Acta* 51 (2005) 125.
- [12] L.A. Kibler, M. Kleinert, R. Randler, D.M. Kolb, *Surface Science* 443 (1999) 19.
- [13] L.A. Kibler, M. Kleinert, D.M. Kolb, *Surface Science* 461 (2000) 155.
- [14] R. Hoyer, L.A. Kibler, D.M. Kolb, *Surface Science* 562 (2004) 275.
- [15] R. Gómez, A. Rodes, J.M. Pérez, J.M. Feliu, A. Aldaz, *Surface Science* 327 (1995) 202.
- [16] J. Clavilier, A. Fernandez-Vega, J.M. Feliu, A. Aldaz, *Journal of Electroanalytical Chemistry* 258 (1989) 89.
- [17] G.A. Attard, A. Bannister, *Journal of Electroanalytical Chemistry* 300 (1991) 467.
- [18] M.J. Llorca, J.M. Feliu, A. Aldaz, J. Clavilier, *Journal of Electroanalytical Chemistry* 351 (1993) 299.
- [19] G.A. Attard, R. Price, A. Al-Akl, *Electrochimica Acta* 39 (1994) 1525.
- [20] J.M. Feliu, B. Alvarez, V. Climent, A. Rodes, in: M.P. Soriaga, J. Stickney, L.A. Bottomley, Y.G. Kim (Eds.), *Thin Films: Preparation, Characterization Applications*, vol. Kluwer Academic/Plenum Publishers, New York, 2002.
- [21] B. Álvarez, A. Rodes, J.M. Pérez, J.M. Feliu, J.L. Rodríguez, E. Pastor, *Langmuir* 16 (2000) 4695.
- [22] J. Clavilier, R. Faure, G. Guinet, R. Durand, *Journal of Electroanalytical Chemistry* 107 (1980) 205.
- [23] N. Hoshi, K. Kagaya, Y. Hori, *Journal of Electroanalytical Chemistry* 485 (2000) 55.
- [24] M. Hara, U. Linke, T. Wandlowski, *Electrochimica Acta* 52 (2007) 5733.
- [25] A. Cuesta, L.A. Kibler, D.M. Kolb, *Journal of Electroanalytical Chemistry* 466 (1999) 165.
- [26] E.D. German, M. Sheintuch, M.K. Alexander, *Journal of Physical Chemistry C* 113 (2009) 15326.
- [27] E.D. German, A.M. Kuznetsov, M. Sheintuch, *Surface Science* 554 (2004) 170.
- [28] B. Álvarez, J.M. Feliu, J. Clavilier, *Electrochemistry Communications* 4 (2002) 379.
- [29] B. Álvarez, A. Rodes, J.M. Pérez, J.M. Feliu, *Journal of Physical Chemistry B* 107 (2003) 2018.
- [30] B. Álvarez, V. Climent, A. Rodes, J.M. Feliu, *Physical Chemistry Chemical Physics* 3 (2001) 3269.
- [31] A. Gil, A. Clotet, J.M. Ricart, F. Illas, B. Álvarez, A. Rodes, J.M. Feliu, *Journal of Physical Chemistry B* 105 (2001) 7263.
- [32] B. Álvarez, V. Climent, A. Rodes, J.M. Feliu, *Journal of Electroanalytical Chemistry* 497 (2001) 125.
- [33] M.J. Ball, C.A. Lucas, N.M. Markovic, V. Stamenkovic, P.N. Ross, *Surface Science* 518 (2002) 201.
- [34] B. Álvarez, A. Berná, A. Rodes, J.M. Feliu, *Surface Science* 573 (2004) 32.
- [35] R. Gómez, A. Rodes, J.M. Pérez, J.M. Feliu, A. Aldaz, *Surface Science* 344 (1995) 85.
- [36] J. Clavilier, D. Armand, S.G. Sun, M. Petit, *Journal of Electroanalytical Chemistry* 205 (1986) 267.
- [37] J. Souza-Garcia, V. Climent, J.M. Feliu, *Electrochemistry Communications* 11 (2009) 1515.
- [38] A. López-Cudero, F.J. Vidal-Iglesias, J. Solla-Gullón, E. Herrero, A. Aldaz, J.M. Feliu, *Journal of Electroanalytical Chemistry* 637 (2009) 63.
- [39] V. Climent, R. Gómez, J.M. Feliu, *Electrochimica Acta* 45 (1999) 629.
- [40] J. Clavilier, R. Albalat, R. Gómez, J.M. Orts, J.M. Feliu, *Journal of Electroanalytical Chemistry* 360 (1993) 325.
- [41] A. Rodes, R. Gómez, J.M. Orts, J.M. Feliu, A. Aldaz, *Journal of Electroanalytical Chemistry* 359 (1993) 315.
- [42] A. Rodes, R. Gómez, J.M. Orts, J.M. Feliu, J.M. Pérez, A. Aldaz, *Langmuir* 11 (1995) 3549.
- [43] R. Gómez, A. Rodes, J.M. Orts, J.M. Feliu, J.M. Pérez, *Surface Science* 342 (1995) L1104.
- [44] A. Rodes, R. Gómez, J.M. Pérez, J.M. Feliu, A. Aldaz, *Electrochimica Acta* 41 (1996) 729.
- [45] F.J. Vidal-Iglesias, A. Al-Akl, D. Watson, G.A. Attard, *Journal of Electroanalytical Chemistry* 611 (2007) 117.
- [46] M.S. Zei, G. Ertl, *Zeitschrift für Physikalische Chemie* 202 (1997) 5.
- [47] M. Duca, V. Kavvadia, P. Rodriguez, S.C.S. Lai, T. Hoogenboom, M.T.M. Koper, *Journal of Electroanalytical Chemistry* 649 (2010) 59.
- [48] V. Rosca, G.L. Beltramo, M.T.M. Koper, *Langmuir* 21 (2005) 1448.
- [49] A. Rodes, V. Climent, J.M. Orts, J.M. Pérez, A. Aldaz, *Electrochimica Acta* 44 (1998) 1077.
- [50] J. Clavilier, J.M. Orts, R. Gómez, J.M. Feliu, A. Aldaz, in: *Proceedings The Electrochemical Society, Pennington*, 94–21, 1994, p. 167.
- [51] V. Climent, G.A. Attard, J.M. Feliu, *Journal of Electroanalytical Chemistry* 532 (2002) 67.
- [52] A.N. Frumkin, O.A. Petrii, *Electrochimica Acta* 20 (1975) 347.
- [53] S.C. Chang, M.J. Weaver, *Surface Science* 230 (1990) 222.